

Cluster Ising quantum batteries can mimic super-extensive charging power

Anna Pavone* and Federico Luigi Cavagnaro*

Dipartimento di Fisica, Università degli studi di Genova, Via Dodecaneso 33, Genova, 16146, Italia

Matteo Carrega

CNR-SPIN, Via Dodecaneso 33, 16146 Genova (Italy)

Riccardo Grazi, Dario Ferraro, and Niccolò Traverso Ziani†

*Dipartimento di Fisica, Università degli studi di Genova, Via Dodecaneso 33, Genova, 16146, Italia and
CNR-SPIN, Via Dodecaneso 33, 16146 Genova (Italy)*

Quantum batteries—miniaturized devices able to store and release energy on demand—are promising both because their intrinsic energy and time scales can match those of other quantum technologies and due to the intriguing possibility of achieving super-extensive charging power. While this enhanced scaling is known to appear in several settings, it is generally believed to be forbidden in Wigner–Jordan integrable spin chains charged via quantum-quench protocols. Here, we show that an extended cluster-Ising model, despite belonging to the above category, exhibits super-extensive charging power over wide ranges of system sizes, reaching up to a thousand spins, in proper parameter regimes. This remarkable anomalous scaling is due to a corresponding super-extensive growth of the stored energy, implying that it occurs at large but finite size and cannot persist in the thermodynamic limit. This phenomenon appears robust against finite-temperature effects.

I. INTRODUCTION

The quest to determine whether quantum technologies can outperform their classical counterparts is one of the main challenges across modern quantum science [1, 2]. Within this vast landscape quantum batteries (QBs), devices devoted to store and release energy exploiting purely quantum effects, offer a fertile ground to explore this question, as they represent a paradigmatic setting in which energetic resources, charging mechanisms and quantum correlations interplay in a fruitful and nontrivial way [3–6].

Among the various figures of merit considered to characterize the performance of these devices, an important role is played by the stored energy and the average charging power, namely the energy which can be delivered to the battery per unit time [7]. In multipartite architectures, composed of N interacting subsystems, the stored energy is typically an extensive quantity, scaling linearly with system size N . Yet what has aroused significant interest is the possibility that the charging power per subsystems might scale in a super-extensive manner, namely $\propto N^\alpha$ with $\alpha > 0$. This behavior indicates that adding cells accelerates the charging process in a way not achievable by independent units [8–11].

Such enhanced scaling may originate from mechanisms that can be collective in nature—which can emerge also in classical or semiclassical systems—or, more interestingly, be due to an actual quantum advantage [12–17].

Notable example within the first category is the so called Dicke QB [18–27], where independent two-, or more generally few-, level systems are charged via the interaction with photons trapped into a resonant cavity. Conversely the emergence of a genuine quantum advantage has been theoretically predicted for the Sachdev–Ye–Kitaev QBs, where a random non-local interaction among the spins can be exploited to reach a super-extensive power [28, 29] and for properly engineered harmonic oscillator QBs with non-linear charger-battery coupling [30].

In spin based QBs [31–35] the possibility to achieve a super-extensive scaling in the power crucially depends on both the range of interaction and the coordination within the lattice formed by the spins [9, 36, 37]. In this context, integrable spin chain QBs have had a major impact in determining robust features of the charging dynamics in the thermodynamic limit [38, 39]. However, due to the fact that their coordination is limited and that they can be mapped into free fermions via Wigner–Jordan transformation [40], it is believed that a super-extensive scaling cannot be observed in this case [13].

In the present paper we will demonstrate that this is indeed not always the case. Focusing on two different versions of the cluster-Ising model [41–43], where the range of interaction can be properly tuned, we will show that there are regions of the parameter space in which a super-extensive scaling for both the stored energy and the power with respect to the number of spin N can be identified. The fact that also the energy scales super-extensively is a clear indication of the fact that this phenomenology can be observed for a large, $O(10^3)$, but finite N . However, it is not expected to survive by properly taking the thermodynamic limit.

The paper is organized as follows. In Section II we dis-

* These authors contributed equally to this work.

† niccolò.traverso.ziani@unige.it

cuss the cluster-Ising model and its solution in terms of Wigner-Jordan transformation and Fourier series. Section III discusses the charging protocol and figures of merit (stored energy and averaged charging power) relevant for the present analysis. The numerical results concerning different possible scaling of the cluster interaction are reported in Section IV, while Section V is devoted to the conclusions. One Appendix shows cases where a

super-extensive power doesn't emerge.

II. UNDERLYING MODELS

As QB Hamiltonians we consider two different versions of the same kind of generalized cluster-Ising model [41–43]. Explicitly we set (up to an overall energy prefactor)

$$H_1 = -\cos\phi_1 \sum_{j=1}^N \sigma_j^x O_{j,n}^z \sigma_{j+n+1}^x + \sin\phi_1 \sum_{j=1}^N \sigma_j^z \quad (1)$$

$$H_2 = -\cos\phi_2 \sum_{j=1}^N \sum_{l=1}^n \frac{1}{n} \sigma_j^x O_{j,l}^z \sigma_{j+l+1}^x + \sin\phi_2 \sum_{j=1}^N \sigma_j^z, \quad (2)$$

with

$$O_{j,n}^z = \prod_{k=1}^n \sigma_{j+k}^z. \quad (3)$$

Here, σ_j^α , ($\alpha = x, y, z$) are the Pauli matrices in the usual representation for the site j , $\phi_{1/2}$ are free real parameters, N is the number of sites composing the chain and $n < N$ is the range of the cluster interaction term. We adopt periodic boundary conditions. The two Hamiltonians under investigation are distinguished by a different form of the multi-spin interaction. In the case of H_1 , a single term with a string of $n+1$ Pauli matrices is present. As far as H_2 is concerned, one has multiple strings of lengths $3, 4, \dots, n+1$, all with the same coefficient in front. The $1/n$ term is introduced to have extensive energies in the thermodynamic limit.

Both models are Wigner-Jordan integrable, meaning that they can be mapped to free fermion models [40]. It is worth to note that a model with different weights in front of each string would also be integrable, but we do not consider it. Explicitly, to solve the models, one first performs the Wigner-Jordan transformation to spinless fermions c_j given by [44]

$$\sigma_j^z = 1 - 2c_j^\dagger c_j, \quad (4)$$

$$\sigma^+ = \prod_{l < j} (1 - 2c_l^\dagger c_l) c_j, \quad (5)$$

$$\sigma^- = \prod_{l < j} (1 - 2c_l^\dagger c_l) c_j^\dagger, \quad (6)$$

with $\sigma_j^\pm = (\sigma_j^x \pm i\sigma_j^y)/2$. Subsequently, to exploit the translational invariance, it is useful to use the Fourier expansion ($q = 0, 1, \dots, N-1$)

$$\psi_q = \frac{1}{\sqrt{N}} e^{-i\frac{\pi}{4}} \sum_{j=1}^N e^{-i\frac{2\pi}{N} q j} c_j \quad (7)$$

to get the Bogoliubov-de Gennes-like form

$$H_{1/2} = \sum_q (\psi_q^\dagger, \psi_{-q}) \mathcal{H}_{1/2}^q (\psi_q, \psi_{-q})^T \quad (8)$$

with

$$\mathcal{H}_{1/2}^q = A_{1/2}^q \tau^z + C_{1/2}^q \tau^x, \quad (9)$$

where $\tau^{z/x}$ are Pauli matrices in a fictitious two-dimensional space and

$$A_1^q = \cos\left(\frac{2\pi}{N}(n+1)q\right) \cos\phi_1 - \sin\phi_1 \quad (10)$$

$$C_1^q = -\sin\left(\frac{2\pi}{N}(n+1)q\right) \cos\phi_1 \quad (11)$$

$$A_2^q = \frac{1}{n} \sum_{p=1}^n \cos\left(\frac{2\pi}{N}(p+1)q\right) \cos\phi_2 - \sin\phi_2 \quad (12)$$

$$C_2^q = -\frac{1}{n} \sum_{p=1}^n \sin\left(\frac{2\pi}{N}(p+1)q\right) \cos\phi_2. \quad (13)$$

Note that, after algebraic manipulations, the terms A_2^q and C_2^q can be rewritten in a compact form as follows

$$A_2^q = \frac{\cos\phi_2}{n} \left[\frac{\sin\left(\frac{(n+1)\theta}{2}\right) \cos\left(\frac{(n+2)\theta}{2}\right)}{\sin(\theta/2)} - \cos\theta \right] - \sin\phi_2,$$

$$C_2^q = -\frac{\cos\phi_2}{n} \left[\frac{\sin\left(\frac{(n+1)\theta}{2}\right) \sin\left(\frac{(n+2)\theta}{2}\right)}{\sin(\theta/2)} - \sin\theta \right],$$

with $\theta = \frac{2\pi}{N}q$. In our derivation, we have restricted the analysis to the odd fermion parity sector, a choice that does not qualitatively alter the results as the Hamiltonians commute with the fermion parity operator and hence the dynamics, which we will consider in the following, is restricted to the same fermion parity sector as the initial state.

III. BATTERY SETUP

The charging of these QBs is implemented via a time-dependent protocol. Specifically, the Hamiltonians $H_{1/2}$ become time-dependent, $H_{1/2}(t)$, through stepwise changes in the angles $\phi_{1/2}$, effectively realizing a double quantum quench [45, 46]. Explicitly

$$\phi_{1/2}(t) = \phi_{1/2}^{(B)}(\Theta(-t) + \Theta(t - \tau)) + \phi_{1/2}^{(C)}\Theta(t)\Theta(-t + \tau), \quad (14)$$

where $\phi_{1/2}^{(B/C)}$ denote respectively the battery and charging parameters, τ is the charging time and $\Theta(\cdot)$ is the Heaviside step function. Correspondingly, one has

$$\begin{aligned} A_{1/2}^q(t) &= A_{1/2}^{q,(B)}(\Theta(-t) + \Theta(t - \tau)) + A_{1/2}^{q,(C)}\Theta(t)\Theta(-t + \tau) \\ C_{1/2}^q(t) &= C_{1/2}^{q,(B)}(\Theta(-t) + \Theta(t - \tau)) + C_{1/2}^{q,(C)}\Theta(t)\Theta(-t + \tau) \end{aligned}$$

]

For $t < 0$ the system is prepared either in the ground state or in a thermal state with temperature $T = 1/(k_B\beta)$, with k_B denoting the Boltzmann constant.

The fundamental figures of merit to characterize these QBs are the energies transferred per spin during the time evolution, referred to as the charging energies. Explicitly, for the two models we have

$$E_{1/2}(\tau) = \frac{\text{Tr}\left[e^{-\beta H_{1/2}(0^-)} \left(H_{1/2}^H(\tau^+) - H_{1/2}^H(0^-)\right)\right]}{N \text{Tr}\left[e^{-\beta H_{1/2}(0^-)}\right]}, \quad (15)$$

where $\text{Tr}[\cdot]$ denotes the trace and $H_{1/2}^H(t)$ are the Hamiltonians in the Heisenberg representation. The calculation of $E_{1/2}(\tau)$ can be performed explicitly and reads as

$$E_{1/2}(\tau) = \sum_q \frac{1 - \cos(2\omega_{1/2}(q)\tau)}{2N\varepsilon_{1/2}(q)\omega_{1/2}^2(q)} \left(C_{1/2}^{q,(B)} A_{1/2}^{q,(C)} - A_{1/2}^{q,(B)} C_{1/2}^{q,(C)}\right)^2 \tanh\left(\frac{\beta\varepsilon_{1/2}(q)}{2}\right). \quad (16)$$

Here,

$$\varepsilon_{1/2}(q) = \sqrt{\left(A_{1/2}^{q,(B)}\right)^2 + \left(C_{1/2}^{q,(B)}\right)^2}, \quad (17)$$

$$\omega_{1/2}(q) = \sqrt{\left(A_{1/2}^{q,(C)}\right)^2 + \left(C_{1/2}^{q,(C)}\right)^2} \quad (18)$$

are the energy dispersions before and during the charging respectively. Notice that the energies do not scale with N in the thermodynamic limit.

The average charging powers $P_{1/2}(\tau)$ follow directly from the energies and are given by

$$P_{1/2}(\tau) = E_{1/2}(\tau)/\tau. \quad (19)$$

For the following analysis, it is useful to introduce the maximal figures of merit. The maximal charging powers $P_{1/2}^M$ are defined as

$$P_{1/2}^M = \max_\tau P_{1/2}(\tau) \quad (20)$$

where the value of τ corresponding to $P_{1/2}^M$ is indicated as τ_{max} . Finally, the maximal energies

$$E_{1/2}^M = E_{1/2}(\tau_{max}) \quad (21)$$

are considered.

IV. RESULTS

While the physics we will discuss is qualitatively independent of $\phi_{1/2}^{(B)/(C)}$, a prominent role is played

by the total number of spins N and by the cluster parameter n . As a first result, in Fig. 1 we show, for $T = 0$, the numerical data of $E_1(\tau)$ (panel (a)) and $E_2(\tau)$ (panel (b)), for various values of N and for fixed n . In the chosen range, the energy per spin clearly increases as the number of spins in the chain increases. Panels (c) and (d) show the same for $P_1(\tau)$ and $P_2(\tau)$. A super-extensive scaling of the charging power is hence present in the considered range. Remarkably, this effect arises not from a favorable scaling of τ_{max} on N like in the Dicke QBs [12, 18, 24], but from the scaling of the stored energy itself.

To better characterize this effect, in Fig. 2 P_1^M and P_2^M are shown in panel (a) and (b) respectively, as a function of N and still at zero temperature. As a guide to the eyes, fits with power laws are superimposed to the numerically evaluated points (blue curves). It is evident a clear super-extensive behavior of the maximum charging power in the considered range of N . Remarkably, the fitting exponent, which is 0.8327 for P_1^M and 0.8933 for P_2^M is close to the evocative value $\alpha = 1$ [8, 9].

A natural question then arises. What happens if we let n scale with N ? Paradigmatic examples in this direction are reported in Fig. 3. Here, results are shown for $n = N^{1/2}$ (panels (a) and (b)) and $n = N^{2/3}$. Although the super-extensive scaling persists, maybe surprisingly, the power law becomes less favorable, being 0.4766 and 0.4989 for the square root case and 0.3015 and 0.3561 for $n = N^{2/3}$.

To conclude, we show in Fig. 4 that the results presented are robust at finite temperature. There,

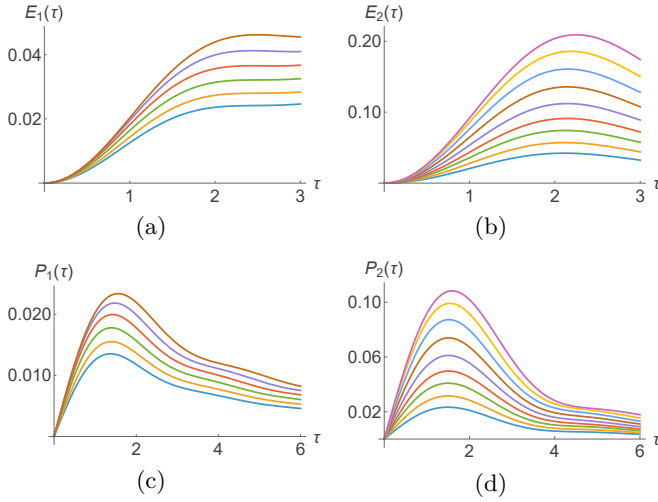


FIG. 1. (Color online) Stored energies per spin $E_1(\tau)$ (a) and $E_2(\tau)$ (b) as a function of the charging time τ and at zero temperature for different values of N (ranging from $N = 169$ to $N = 324$ for (a) and from $N = 36$ to $N = 196$ for (b)) and at fixed $n = 15$. Averaged charging power per spin $P_1(\tau)$ (c) and $P_2(\tau)$ (d) as a function of the charging time τ and at zero temperature for different values of N (ranging from $N = 169$ to $N = 324$ for (c) and from $N = 36$ to $N = 196$ for (d)) and at fixed $n = 15$.

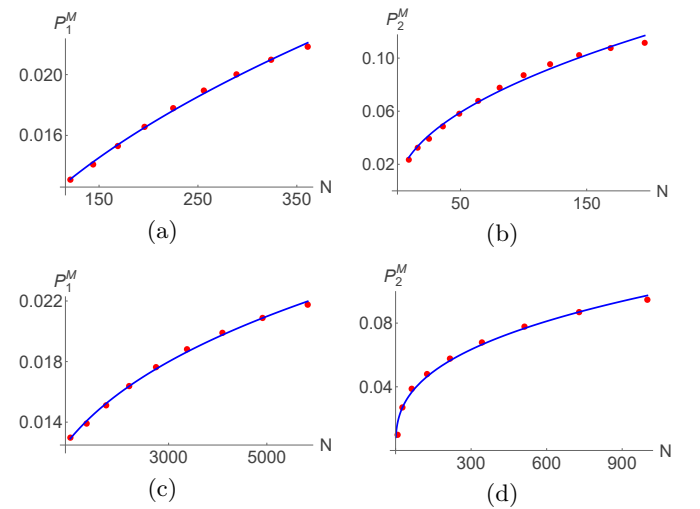


FIG. 3. (Color online) Best fit of P_1^M (left panels) and P_2^M (right panels) in the form $P_{1/2}^M = a_{1/2}N^{\alpha_{1/2}}$ for: the case $n = N^{1/2}$ (a-b), the blue curves corresponding to $(a_1 \approx 0.0013, \alpha_1 \approx 0.4766)$ and $(a_2 \approx 0.0084, \alpha_2 \approx 0.4989)$ respectively; $n = N^{2/3}$ (c-d), the blue curves corresponding to $(a_1 \approx 0.0016, \alpha_1 \approx 0.3015)$ and $(a_2 \approx 0.0083, \alpha_2 \approx 0.3561)$ respectively.

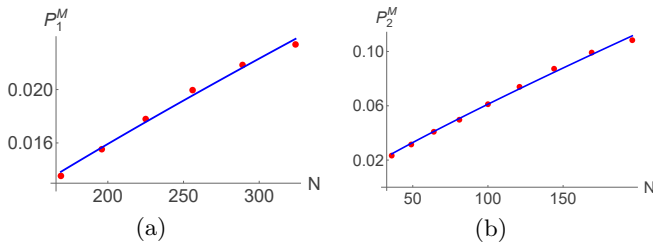


FIG. 2. (Color online) Best fit of P_1^M (a) and P_2^M (b) extracted from Fig. 1 (c) and (d) in the form $P_{1/2}^M = a_{1/2}N^{\alpha_{1/2}}$. The blue curves correspond to $(a_1 \approx 0.00019, \alpha_1 \approx 0.8327)$ and $(a_2 \approx 0.001, \alpha_2 \approx 0.8933)$ respectively.

the same quantities of Fig. 2 and Fig. 3 are reported for $\beta = 1$, showing a qualitative agreement with the zero temperature scenario. Significant cases where the discussed super-extensive behavior does not occur are reported in the Appendix.

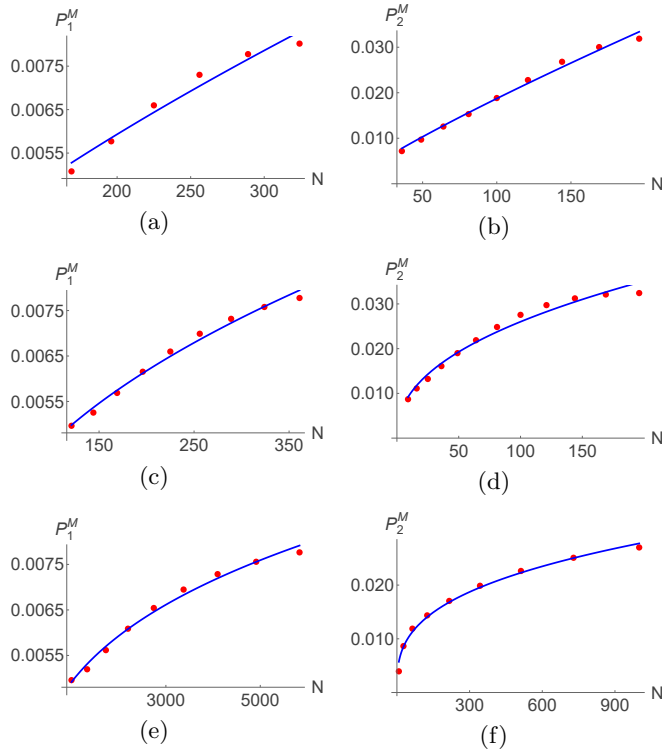


FIG. 4. (Color online) Best fit of P_1^M (left panels) and P_2^M (right panels) in the form $P_{1/2}^M = a_{1/2}N^{\alpha_{1/2}}$ for: fixed $n = 15$ (a-b), the blue curves corresponding to $(a_1 \approx 0.00015, \alpha_1 \approx 0.6943)$ and $(a_2 \approx 0.00036, \alpha_2 \approx 0.8595)$ respectively; the case $n = N^{1/2}$ (c-d), the blue curves corresponding to $(a_1 \approx 0.00064, \alpha_1 \approx 0.4275)$ and $(a_2 \approx 0.0035, \alpha_2 \approx 0.4326)$ respectively; the case $n = N^{2/3}$ (e-f), the blue curves corresponding to $(a_1 \approx 0.00076, \alpha_1 \approx 0.2699)$ and $(a_2 \approx 0.0029, \alpha_2 \approx 0.3272)$ respectively. All the plots are done at the same fixed inverse temperature $\beta = 1$.

V. CONCLUSIONS

We have investigated the charging performance of quantum batteries based on two Wigner-Jordan integrable extensions of the cluster-Ising spin chain. Despite the integrability of both models, we have shown that they can exhibit an apparent super-extensive scaling of the charging power across wide intervals of system sizes, reaching up to $O(10^3)$ spins. Our analysis demonstrates that this behavior does not originate from an anomalous dependence of the optimal charging time on the system size, but rather from a super-extensive growth of the stored energy itself. As such, the effect cannot persist in the thermodynamic limit and should instead be interpreted as a finite-size enhancement. Similar behaviors characterize both the constant n case, and the regime

in which n scales with N . Finally, we verified that the phenomenon is robust against thermal effects, which affect quantitative values but not the qualitative trends. This analysis seems to suggest a scaling of the averaged charging power per spin of the form $P_{1/2}^M \propto N/n$, even if a more detailed investigation, for example addressing possible full analytical solutions, are needed.

Altogether, our results highlight that even fermionic integrable models—typically considered incapable of supporting enhanced charging power under quench protocols [13]—can display strong finite-size effects mimicking super-extensive performance. These findings can help delineate the boundaries between genuine collective advantages and finite-size artifacts in quantum battery architectures.

Appendix: Unfavorable regimes

In this appendix we show two representative regimes where the super-extensive scaling is not observed. They are reported in Fig. 5. Panel (a) shows a range of N in which the charging power approaches the extensive regime, while in panel (b) the case of $n = N^{1/3}$ is reported. In this latter case, the dependence on N of the charging power is pronounced, but a sub-extensive scaling emerges in the considered range of systems sizes N .

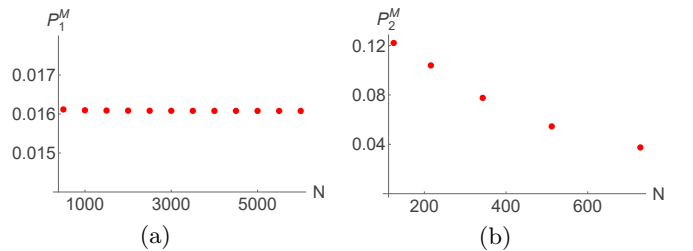


FIG. 5. (Color online) Behavior of P_1^M for $n = N/2$ (a) and P_2^M for $n = N^{1/3}$ (b) at zero temperature.

ACKNOWLEDGMENTS

D.F. acknowledge support from the project PRIN 2022 - 2022XK5CPX (PE3) SoS-QuBa - "Solid State Quantum Batteries: Characterization and Optimization" funded within the programme "PNRR Missione 4 - Componente 2 - Investimento 1.1 Fondo per il Programma Nazionale di Ricerca e Progetti di Rilevante Interesse Nazionale (PRIN)", funded by the European Union - Next Generation EU".

[1] O. Ezratty, *Understanding Quantum Technologies* (2024), arXiv:2111.15352 [quant-ph].

[2] R. Aguado, R. Citro, M. Lewenstein, and M. Stern, *New Trends and Platforms for Quantum Technologies*, Lecture

Notes in Physics Vol. 1025 (Springer Nature Switzerland, Cham, 2024).

[3] J. Q. Quach, G. Cerullo, and T. Virgili, Quantum batteries: The future of energy storage?, *Joule* **7**, 2195 (2023).

[4] F. Campaioli, S. Gherardini, J. Q. Quach, M. Polini, and G. M. Andolina, Colloquium: Quantum batteries, *Rev. Mod. Phys.* **96**, 031001 (2024).

[5] A. Camposeo, T. Virgili, F. Lombardi, G. Cerullo, D. Pisignano, and M. Polini, Quantum batteries: A materials science perspective, *Adv. Mater.* **37**, 2415073 (2025).

[6] D. Ferraro, F. Cavaliere, M. G. Genoni, G. Benenti, and M. Sassetti, Opportunities and challenges of quantum batteries, *Nat. Rev. Phys.* (2026), doi:10.1038/s42254-025-00906-5.

[7] G. M. Andolina, D. Farina, A. Mari, V. Pellegrini, V. Giovannetti, and M. Polini, Charger-mediated energy transfer in exactly solvable models for quantum batteries, *Phys. Rev. B* **98**, 205423 (2018).

[8] F. C. Binder, S. Vinjanampathy, K. Modi, and J. Goold, Quantacell: Powerful charging of quantum batteries, *New J. Phys.* **17**, 075015 (2015).

[9] F. Campaioli, F. A. Pollock, F. C. Binder, L. Céleri, J. Goold, S. Vinjanampathy, and K. Modi, Enhancing the charging power of quantum batteries, *Phys. Rev. Lett.* **118**, 150601 (2017).

[10] L. Gao, C. Cheng, W.-B. He, R. Mondaini, X.-W. Guan, and H.-Q. Lin, Scaling of energy and power in a large quantum battery-charger model, *Phys. Rev. Res.* **4**, 043150 (2022).

[11] C.-K. Hu, C. Liu, J. Zhao, L. Zhong, Y. Zhou, M. Liu, H. Yuan, Y. Lin, Y. Xu, G. Hu, G. Xie, Z. Liu, R. Zhou, Y. Ri, W. Zhang, R. Deng, A. Saguia, X. Linpeng, M. S. Sarandy, S. Liu, A. C. Santos, D. Tan, and D. Yu, Quantum charging advantage in superconducting solid-state batteries, *Phys. Rev. Lett.* **136**, 060401 (2026).

[12] G. M. Andolina, M. Keck, A. Mari, V. Giovannetti, and M. Polini, Quantum versus classical many-body batteries, *Phys. Rev. B* **99**, 205437 (2019).

[13] S. Julià-Farré, T. Salamon, A. Riera, M. N. Bera, and M. Lewenstein, Bounds on the capacity and power of quantum batteries, *Phys. Rev. Res.* **2**, 023113 (2020).

[14] G. Francica, Quantum correlations and ergotropy, *Phys. Rev. E* **105**, L052101 (2022).

[15] J.-Y. Gyhm and U. R. Fischer, Beneficial and detrimental entanglement for quantum battery charging, *AVS Quantum Sci.* **6**, 012001 (2024).

[16] A. Hokkyo and M. Ueda, Universal upper bound on ergotropy and no-go theorem by the eigenstate thermalization hypothesis, *Phys. Rev. Lett.* **134**, 010406 (2025).

[17] F. Cavaliere, D. Ferraro, M. Carrega, G. Benenti, and M. Sassetti, Quantum advantage bounds for a multipartite Gaussian battery, arXiv:2510.24162 [quant-ph] (2025).

[18] D. Ferraro, M. Campisi, G. M. Andolina, V. Pellegrini, and M. Polini, High-power collective charging of a solid-state quantum battery, *Phys. Rev. Lett.* **120**, 117702 (2018).

[19] G. Gemme, G. M. Andolina, F. M. D. Pellegrino, M. Sassetti, and D. Ferraro, Off-resonant Dicke quantum battery: Charging by virtual photons, *Batteries* **9**, 202 (2023).

[20] J. Q. Quach, K. E. McGhee, L. Ganzer, D. M. Rouse, B. W. Lovett, E. M. Gauger, J. Keeling, G. Cerullo, D. Lidzey, and T. Virgili, Superabsorption in an organic microcavity: Toward a quantum battery, *Sci. Adv.* **8**, eabk3160 (2022).

[21] J. Carrasco, J. R. Maze, C. Hermann-Avigliano, and F. Barra, Collective enhancement in dissipative quantum batteries, *Phys. Rev. E* **105**, 064119 (2022).

[22] L. Wang, S.-Q. Liu, F.-L. Wu, H. Fan, and S.-Y. Liu, Deep strong charging in a multiphoton anisotropic Dicke quantum battery, *Phys. Rev. A* **110**, 042419 (2024).

[23] D.-L. Yang, F.-M. Yang, and F.-Q. Dou, Three-level Dicke quantum battery, *Phys. Rev. B* **109**, 235432 (2024).

[24] A. Canzio, V. Cavina, M. Polini, and V. Giovannetti, Single-atom dissipation and dephasing in Dicke and Tavis-Cummings quantum batteries, *Phys. Rev. A* **111**, 022222 (2025).

[25] D. J. Tibben, E. Della Gaspera, J. van Embden, P. Reineck, J. Q. Quach, F. Campaioli, and D. E. Gómez, Extending the self-discharge time of Dicke quantum batteries using molecular triplets, *PRX Energy* **4**, 023012 (2025).

[26] Y. Kurman, K. Hymas, A. Fedorov, W. J. Munro, and J. Quach, Powering quantum computation with quantum batteries, *Phys. Rev. X* **16**, 011016 (2026).

[27] K. Hymas *et al.*, Experimental demonstration of a scalable room-temperature quantum battery, arXiv:2501.16541 [quant-ph] (2025).

[28] D. Rossini, G. M. Andolina, D. Rosa, M. Carrega, and M. Polini, Quantum advantage in the charging process of Sachdev-Ye-Kitaev batteries, *Phys. Rev. Lett.* **125**, 236402 (2020).

[29] D. Rosa, D. Rossini, G. M. Andolina, M. Polini, and M. Carrega, Ultra-stable charging of fast-scrambling SYK quantum batteries, *J. High Energy Phys.* **2020**, 067 (2020).

[30] G. M. Andolina, V. Stanzione, V. Giovannetti, and M. Polini, Genuine quantum advantage in anharmonic bosonic quantum batteries, *Phys. Rev. Lett.* **134**, 240403 (2025).

[31] T. P. Le, J. Levinsen, K. Modi, M. M. Parish, and F. A. Pollock, Spin-chain model of a many-body quantum battery, *Phys. Rev. A* **97**, 022106 (2018).

[32] D. Rossini, G. M. Andolina, and M. Polini, Many-body localized quantum batteries, *Phys. Rev. B* **100**, 115142 (2019).

[33] S. Ghosh, T. Chanda, and A. Sen(De), Enhancement in the performance of a quantum battery by ordered and disordered interactions, *Phys. Rev. A* **101**, 032115 (2020).

[34] M. B. Arjmandi, H. Mohammadi, and A. C. Santos, Enhancing self-discharging process with disordered quantum batteries, *Phys. Rev. E* **105**, 054115 (2022).

[35] A. Catalano, S. Giampaolo, O. Morsch, V. Giovannetti, and F. Franchini, Frustrating quantum batteries, *PRX Quantum* **5**, 030319 (2024).

[36] J.-Y. Gyhm, D. Šafránek, and D. Rosa, Quantum charging advantage cannot be extensive without global operations, *Phys. Rev. Lett.* **128**, 140501 (2022).

[37] A. Ali *et al.*, Kitaev quantum batteries: Superextensive scaling of ergotropy in a 1D spin-1/2 XY- γ chain, arXiv:2411.14074 [quant-ph] (2024).

[38] R. Grazi, D. Sacco Shaikh, M. Sassetti, N. Traverso Ziani, and D. Ferraro, Controlling energy storage crossing quantum phase transitions in an integrable spin quantum battery, *Phys. Rev. Lett.* **133**, 197001 (2024).

- [39] R. Grazi, F. Cavaliere, M. Sassetto, D. Ferraro, and N. Traverso Ziani, Charging free fermion quantum batteries, *Chaos Solitons Fractals* **196**, 116383 (2025).
- [40] F. Franchini *et al.*, *An Introduction to Integrable Techniques for One-Dimensional Quantum Systems*, Lecture Notes in Physics Vol. 940 (Springer, 2017).
- [41] P. Smacchia, L. Amico, P. Facchi, R. Fazio, G. Florio, S. Pascazio, and V. Vedral, Statistical mechanics of the cluster Ising model, *Phys. Rev. A* **84**, 022304 (2011).
- [42] C. Ding, Phase transitions of a cluster Ising model, *Phys. Rev. E* **100**, 042131 (2019).
- [43] S. Kheiri, R. Jafari, S. Mahdavifar, S. E. N. Oskooee, and A. Akbari, Dynamical phase diagram of the quantum Ising model with cluster interaction under noiseless and noisy driven field, *Sci. Rep.* **15**, 44339 (2025).
- [44] P. Jordan and E. Wigner, Über das Paulische Äquivalenzverbot, *Z. Phys.* **47**, 631 (1928).
- [45] A. Mitra, Quantum quench dynamics, *Annu. Rev. Condens. Matter Phys.* **9**, 245 (2018).
- [46] S. Porta, F. Cavaliere, M. Sassetto, and N. Traverso Ziani, Topological classification of dynamical quantum phase transitions in the XY chain, *Sci. Rep.* **10**, 12766 (2020).